Journal of Engineering Science and Technology
Vol. 17, No. 1 (2022) 0106 - 0126

EFFECT OF HULL DESIGN VARIATIONS ON THE RESISTANCE PROFILE AND WAVE PATTERN: A CASE STUDY OF THE PATROL BOAT VESSEL

ADITYA RIO PRABOWO[1,*], EVAN MARTONO[1], TEGUH MUTTAQIE[2], TUSWAN TUSWAN[3], DONG MYUNG BAE[4]

[1]Department of Mechanical Engineering, Universitas Sebelas Maret, Surakarta 57126, Indonesia
[2]Agency for the Assessment and Application of Technology, Jakarta 10340, Indonesia
[3]Department of Naval Architecture, Universitas Diponegoro, Semarang 50275, Indonesia
[4] Department of Naval Architecture and Marine Systems Engineering, Pukyong National University, Busan 48513, South Korea
*Corresponding Author: aditya@ft.uns.ac.id

Abstract

Indonesia is a country with large amount of territorial water of around 3.25 million km^2, which requires reliable vehicles to oversee the Indonesian sea area to guard its sovereignty. One potential solution is to deploy high-speed patrol boats that have high efficiency in traversing the Indonesian sea. Due to the large territorial size and Indonesian sea waves, research on hydrodynamic characteristics is crucial. In this research, we investigated the critical parameters in a high-speed vessel to reduce the drag coefficient of the wet surface area. Several hull designs are proposed in this work with a variety in hull types, i.e., monohull and catamaran. A deadrise angle in the range of 10°-30° was also considered as a geometric parameter. To quantify the effect of the resistance phenomenon, we varied the Froude number in the calculations. We used a numerical method to obtain the investigation results with the Savitsky mathematical model. Our initial results indicated that the design with a large deadrise angle showed lower drag compared to the reference boat design, which followed the superiority of the catamaran. In monohull planing, we found that the hull resistance decreased by 16.87% at a 30° deadrise angle compared to the most significant resistance at any other deadrise angle. In catamaran planing, we found that the hull resistance decreased by 7.8% at the 30° deadrise angle compared to the most significant resistance at other angles.

Keywords: Catamaran, Deadrise angle, High-speed vessel, Monohull, Patrol boat, Ship resistance.

1. Introduction

Indonesia is an archipelagic maritime country that has a large area with an estimated 17,000 islands spread over the Indonesian territory [1]. With a population of 255.18 million people spread across various islands, more than 50% of Indonesia's population lives on Java, and Java is the axis of the Indonesian economy [2]. The logistics distribution process from Java to various other islands is one of the main factors of the success of the Indonesian economy. Using sea transportation to reach other islands is a strategic issue in the distribution of logistics [3]. Using sea transportation has the threat of crime from specific groups, such as piracy, smuggling, and kidnapping [4]. The maritime crime cases in Indonesia in 2018 reached a total of 27 cases [5]. In 2018, incidents with bulk carrier vessels reached 74%, while, in 2007-2017, incidents occurred in tankers for 43% of cases, bulk carriers for 34% of cases, and container ships for 7.2% of cases [5]. Based on this data, logistical vehicles, such as tankers, bulk carriers, and container ships, experience a high crime threat. Increasing maritime security is a top priority, for instance regular patrols, and the response time of the arrival of officers at the location becomes a determining factor for reducing maritime crime rates. The Indonesian government created an Integrated Fleet System that is focused on strengthening submarines, frigates, and patrols following the Minimum Essential Force (MEF) 2024.

The solution is to deploy a high-speed patrol boat near the Indonesian borders. A high-speed patrol boat can increase the time efficiency. An investigation regarding the hydrodynamics of the hulls is critical. A few years ago, a study on high-speed vessels was focused on how to reduce drag force on the hull surface [6]. Several hull types are used for the research, and modifications were included. The typical design of the high-speed vessel involves a planing hull or a planing catamaran for military and patrol vessels [6-8]. Hull modifications can be applied to make the hull more hydrodynamic, which reduces the hull resistance. One is the modification of the deadrise angle; the deadrise angle can optimize the ability of the hull to minimize resistance characteristics [9]. The effect of resistance is commonly investigated using numerical analysis (regression and computational fluid dynamics [10-15]) and also analytical calculations, i.e., the Savitsky and Holtrop formulae [16-20].

Selecting a correct deadrise angle can help to stabilize the hull and facilitate a smoother ride. This also reduces the wetted area and drag in the planing hull. Considering the necessity of development in the military field, especially in maritime areas against the mentioned threats and dangers, design of patrol boat has to be sustainably improved. Geometrical design modifications have almost limitless possibilities, which must be quantified regarding the effects on the performance of patrol boat design.

This research is focussed on the value of a ship's hull resistance followed by a change in the deadrise angle, by comparing two types of hulls: the planing hull (monohull) and planing catamaran. In this paper, we used the Savitsky mathematical model to quantify effect of the modifications on the designed hulls to the resistance characteristics. To ensure the resistance calculation validity, the Savitsky mathematical model in numerical analysis was validated with the analytical solutions. The effect of resistance is also discussed based on the variety of the Froude number (F_n) to summarise its influence regarding the significance of the formed wave pattern.

2. Theoretical Basis

2.1. Resistance definition

A boat that is moving forward on the water will have a force aimed in the opposite direction of the ship. Resistance is a characteristic parameter about the hydrodynamics of the hull [21]. There are many types of resistance including friction, wave-making, and hull form drags. Resistance is influenced by several factors, such as the ship speed (V_s), displacement, and hull shape [22]. Based on the forces that affect this, resistance can be divided into normal and tangential forces on the hull (see Fig. 1). The total resistance can be considered as shown in Eq. (1).

$$R_T = R_F + R_V + R_W \tag{1}$$

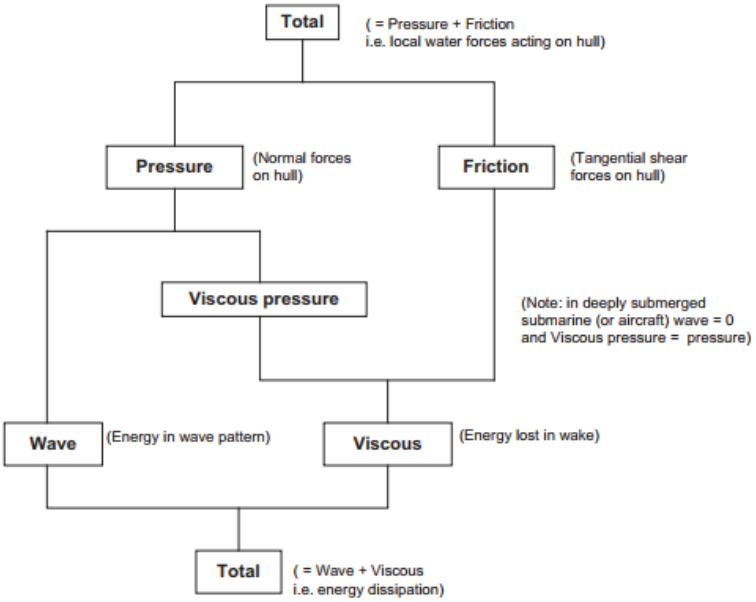

Fig. 1. Classification of small-angle stability.

2.1.1. Frictional resistance

Frictional resistance is a component of the resistance related to the energy released due to the influence of fluid viscosity (a consequence of the water friction on the ship's body). The primary causes of this resistance are the viscosity, ship speed, and wet area surface [21]. The wetted surface is affected by the tangential pressure along the direction of motion of the ship [23]. The general formula for the ship's friction resistance is given by Eq. (2), and the coefficient of friction from International Towing Tank Conference (ITTC) 1975 is given by Eq. (3).

$$Rf = \frac{1}{2}\rho . Cf . S . V^2 \tag{2}$$

$$Cf = \frac{0.075}{(LogRe-2)^2} \tag{3}$$

2.1.2. Viscous resistance

The value of the viscous resistance depends on the viscous form factor (1+k), for a monohull, and (1+βk) [21]. Viscous resistance is the effect of two-dimensional approach friction together against particles and a liquid [24]. This resistance is partly from the normal pressure force on the hull and is also partly from the resistance friction. The coefficient of viscous resistance can be considered, as shown in Eq. (4).

$$Cv=(1+k)\,Cf \tag{4}$$

2.1.3. Wave resistance

The wave resistance (R_W) can be considered zero at high speeds due to minimal resistance values (see Eq. (5)) [21]. If the Froude number reaches 0.89, the wave resistance can be ignored because the value is too small, and the component resistance of the ship will be more affected by the frictional resistance in the wetted surface area [25]. At the Froude number 0.89, the ship begins to enter the planing phase [26].

$$R_W=c_1c_2c_5\,\nabla\rho g exp\{m_1Fr^d+m_4\,cos(\lambda F_r^{-2})\} \tag{5}$$

2.1.4. Reynold's number

From the Reynold's number, we know the form of the fluid. The Reynold's number is one of the parameters used to identify different fluids as laminar or turbulent. The Reynold number equation is the ratio between the force of inertia and the viscosity (see Eq. (6)). A flow can be said to be a laminar flow if the Reynold's number is between 2300 and 4000 and can be said to be turbulent if the Reynold's number is above 4000 [27].

$$Rn=\frac{V.L}{v} \tag{6}$$

2.1.5. Froude number

A Froude number is a dimensionless number used in hydrodynamics to indicate how well a particular model works for a whole system. The Froude number represents the speed compared to the displacement mass (see Eq. (7)) [21]. Froude numbers can be classified into several types. When the Froude number is between 0.4 and 1, the system is said to be semi-displacement; if it is above 1, the system is categorized as a planing hull [26].

$$Fn=\frac{V}{\sqrt[2]{g.LWL}} \tag{7}$$

2.1.6. Wetted surface area

Mumford's formula for finding a wetted surface area has an error rate of approximately 7% [23]. To improve the accuracy of methods, researchers have carried out using configurations for certain types of ships. The wetted surface area can affect the total resistance of a ship. A smaller number of wetted surface areas will reduce the total resistance of the ship [28]. The wetted surface area can be considered as shown in Eq. (8).

$$S=1.025.\,Lpp.\,(Cb.b+1.7\,T) \tag{8}$$

2.1.7. Savitsky total resistance

Daniel Savitsky published about ship hydrodynamics with an estimation of the ship's resistance and trim angle on a ship [29]. Daniel Savitsky's formula was obtained from empirical data on prismatic planing hulls (see Eq. (9)) [9].

$$RT = \Delta \tan\tau + \frac{\frac{1}{2}\rho V^2 \lambda b^2 Cf}{\cos\tau} \quad (9)$$

2.2. Deadrise angle

The deadrise is angle measured in the section plane between the hull and the horizontal, and it is measured at midship [30] (see Fig. 2). The effect of changing the deadrise angle affects the trim angle, where the smaller the rise of the deadrise angle, the smaller the trim angle. The deadrise angle also affects the stability of the ship, at low speeds, and high trim angles can interfere with the transversal stability of the ship [9].

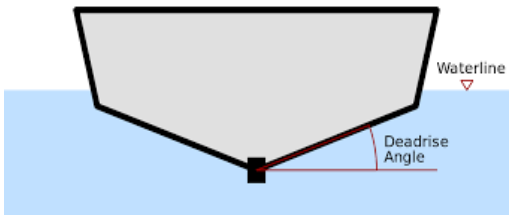

Fig. 2. Geometric scheme of the deadrise angle.

3. Desain and Numerical Configuration

3.1. Main dimensions and hull ratio

In this design process, to determine the size of the ship, we used the comparison ship ratio method for the main dimensions of the ship by following the rules that apply to the KKCTBN Competition in Indonesia. There were two types of comparison ships used, each of which with the same ship characteristics and hull shape. For the planing monohull and planing catamaran, each type had five vessels compared.

The main dimension values on the comparison vessel and their means are shown in Tables 1 and 2 (HSSV: High Speed Support Vessel; JHSV: Joint High Speed Vessel; TSV: Theatre Support Vessel). From the tables, we obtained the main comparisons on the ship, namely *L/B*, to determine the shape of the slender hull or not. The greater the value of *L/B*, the better the characteristics of the ship will be for high speed; however, the ability for the ship to manoeuvre is reduced. The *L/H* ratio affects the longitudinal strength of the ship. The *B/T* ratio will have an impact on the stability of the ship and the position of the ship's equilibrium points.

The prototype had a planing hull, because this is suitable for ships in the fast category. A planing hull has a V-shape, and a planing catamaran is useful for reducing the slamming in a rough sea. The dimensions of the ships were adjusted to the ratio of the actual ships, using a comparison of five fast ships each of the planing hull and planing catamaran types. We obtained $L/B = 3.56$, $L/H = 7.09$, and $B/T = 4.2$ for the planing hulls; and $L/B = 3.43$, $L/H = 12.56$, and $B/T = 6$ for the

planing catamarans. Table 3 represents the dimension characteristics for the planing hull and planing catamaran types. The monohull planing and the catamaran planing ship models are displayed in Figs. 3 and 4.

Table 1. Reference data of existing patrol boats: monohull.

Principal Dimension	Austal Patrol 22 (m)	Austal Patrol 21 (m)	Austal Patrol 22 Kuwait (m)	Stan Patrol 1650 (m)	Austal Patrol 16 (m)	Average (m)
L_{OA}	21.2	21.2	21.6	16.5	17	19.5
L_{WL}	17.9	17.8	19.6	15.3	14.2	16.96
Beam	5.5	5.5	6	5.4	4.9	5.46
Depth	3.3	2.8	3.6	1.8	2.7	2.84
Draught	1.7	1.83	1.5	0.8	1.2	1.406

Table 2. Reference data of existing patrol boats: catamaran.

Principal Dimension	Austal HSSV 72 (m)	Austal JHSV (m)	Austal TSV 101 (m)	Ratayapiban bacha (m)	Reef Ranger (m)	Average (m)
L_{OA}	72.5	103	101	26.62	23.99	65.422
L_{WL}	-	-	86.2	24.7	24.8	45.23333
Beam	18.66	28.15	26.7	8.5	8.5	18.102
Depth	5	6.2	9.4	1.8	3.6	5.2
Draft	3	3.83	4.3	1.5	1.9	2.906

Table 3. Summary of the test model specifications.

Parameters	Monohull	Catamaran	Units
L_{OA}	0.7	0.7	m
L_{WL}	0.7	0.7	m
B	0.196	0.204	m
T	0.0468	0.034	m

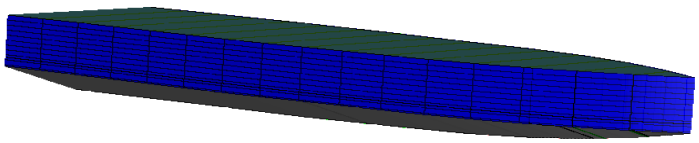

Fig. 3. Design of the monohull patrol boat.

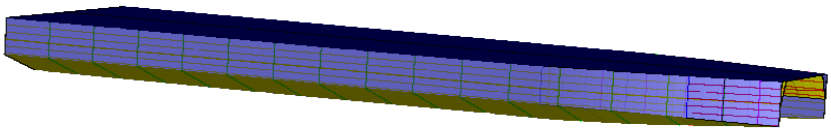

Fig. 4. Design of the catamaran patrol boat.

3.2. Design variations

The design was performed with numerical calculation and analytical method according to concept of the Savitsky's mathematical model. The design parameters were predetermined using the actual ship comparisons as discussed in previous sub-section. After obtaining a comparison of the actual vessels, the details of the dimension parameters are in Table 4 for planing monohulls, and Table 5 for planing catamarans with different deadrise angles. The controlled variable was the speed from 5 to 10, 15, 20, 25, and 30 knots.

Table 4. Details of the principal dimension: monohull design with variation on the deadrise angles.

Symbol	Value					Unit
β	10	15	20	25	30	°
L_{OA}	0.7	0.7	0.7	0.7	0.7	m
L_{WL}	0.7	0.7	0.7	0.7	0.674	m
B	0.196	0.196	0.196	0.196	0.161	m
T	0.0468	0.0468	0.0468	0.0468	0.0468	m
C_M	0.814	0.719	0.616	0.509	0.5	-
C_P	0.885	0.879	0.871	0.859	0.878	-
C_B	0.72	0.632	0.537	0.437	0.439	-
∇	0.005	0.004	0.003	0.003	0.002	m^3
Δ	0.00474	0.004153	0.003539	0.00288	0.002291	tonnes
S	0.139317	0.14204	0.1460052	0.151383	0.125301	m^2

Table 5. Details of the principal dimension: catamaran design with variation on the deadrise angles.

Symbol	Value					Unit
β	10	15	20	25	30	°
L_{OA}	0.7	0.7	0.7	0.7	0.7	m
L_{WL}	0.7	0.7	0.7	0.7	0.674	m
B	0.204	0.204	0.204	0.204	0.161	m
T	0.034	0.034	0.034	0.034	0.034	m
C_M	0.656	0.620	0.618	0.543	0.449	-
C_P	0.85	0.85	0.871	0.852	0.853	-
C_B	0.557	0.527	0.538	0.462	0.426	-
∇	0.003	0.003	0.003	0.002	0.002	m^3
Δ	0.002774	0.002624	0.003539	0.002302	0.00212	tonnes
S	0.145003	0.147838	0.1519646	0.15292	0.140031	m^2

Deadrise angle configuration

Any changes to the deadrise angle will result in a sharper hull shape (see Table 6). The change in the deadrise angle will make the contour of the waterline turn higher. Variation was conducted on the deadrise angle every 5° to determine the effect of each change that occurs. The catamaran hulls were divided into two types, namely, symmetrical and asymmetrical. Both have different hydrodynamic forms and properties. Symmetrical catamarans generally have smaller drag values [31]. In catamaran planing, every increase in the deadrise angle will reduce the coefficient of lift [20].

Table 6. Variations in hull and deadrise angle.

Deadrise Angle (°)	Type of Hull	
	Monohull	**Catamaran**
10	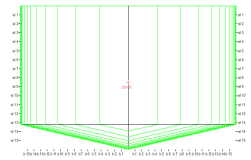	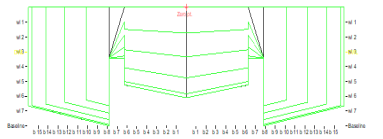
15	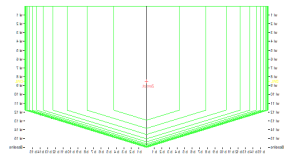	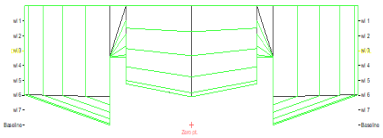
20	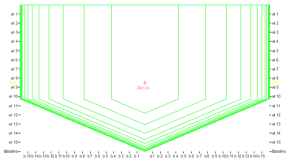	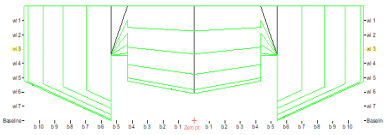
25	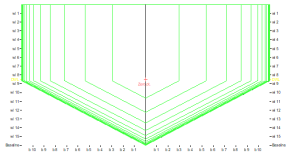	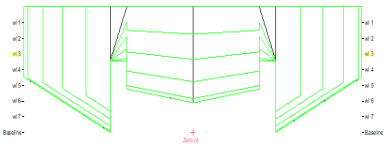
30	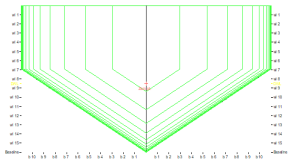	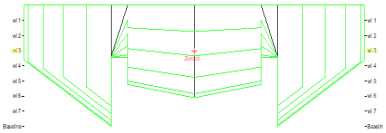

3.3. Numerical configurations

In this section, the hydrostatic data of the ship is seen as an independent variable of each ship's configuration. The movement speed of the ship is a controlled variable with a minimum speed of 5 knots and a maximum of 30 knots. Based on the ITTC 1975, the configuration was as follows: kinematic viscosity 0.0000011 m^2/s, density of water = 1025 kg/m^3, gravity 9.8 m/s^2, saltwater (3.5% salinity), and water temperature 15 °C.

4. Results and Discussion

4.1. Resistance characteristic

The hull resistance consists of the frictional force due to the tangential force and the pressure force consisting of the viscous force and the wave force due to the normal force [21, 32]. A semi-empirical Savitsky method can be used in the planing hull, and the method was obtained based on experiments using a prismatic planing hull [29]. However, the Savitsky method can also be used in other hull types in addition to the planing hull; several studies have shown that this method can be used in multihulls [33]. Through the Savitsky method, the resistance, trim angle, and stability of the ship can be determined [29]. As presented in Fig. 5, there are differences in each deadrise angle from planing monohulls, using numerical comparisons with the simulation results showing an error difference below 10%.

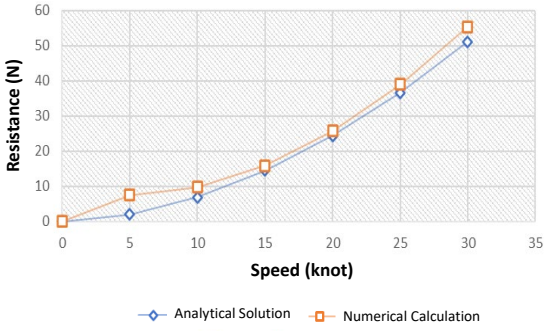

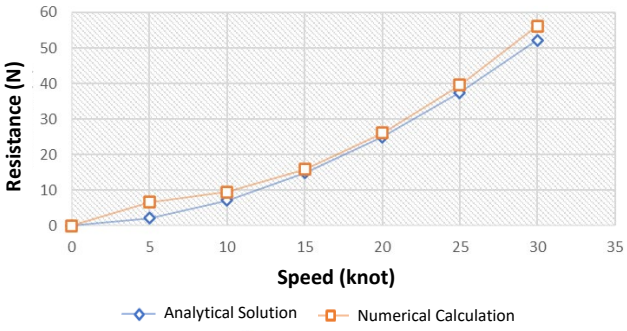

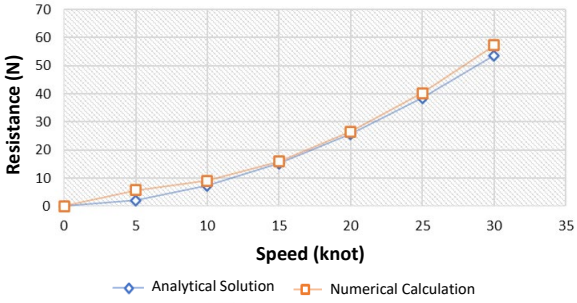

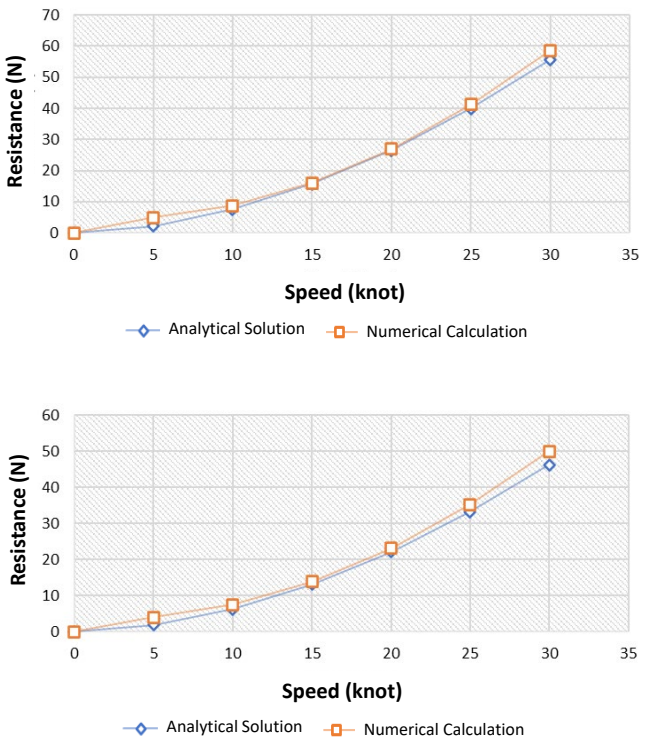

Fig. 5. Correlation speed with the resistance planing monohull.

From Fig. 5(a), we found the highest resistance value of 51.17 N at 30 knots in speed; in Fig. 5(b), the highest resistance is 52.18 N; in Fig. 5(c), the highest resistance is 53.63 N; in Fig. 5(d), the highest resistance is 55.61 N; and in Fig. 5(e), the highest resistance is 46.22 N. The most significant error at speeds of 5 knots was above 50%, and above 10% at speeds of 10 knots, on every change of deadrise angle. On the other hand, as seen in Fig. 6, there were differences in each deadrise angle with the planing monohull, using numerical comparisons with the simulation results show an error difference below 10%.

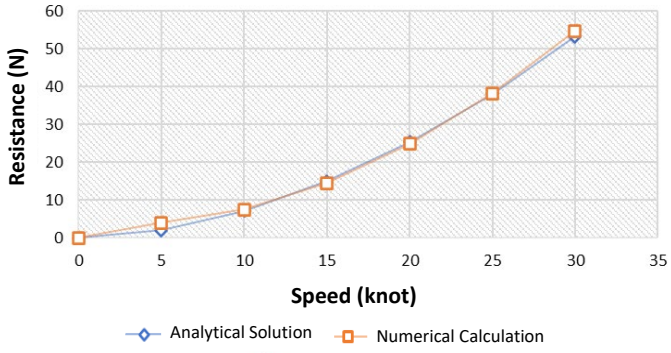

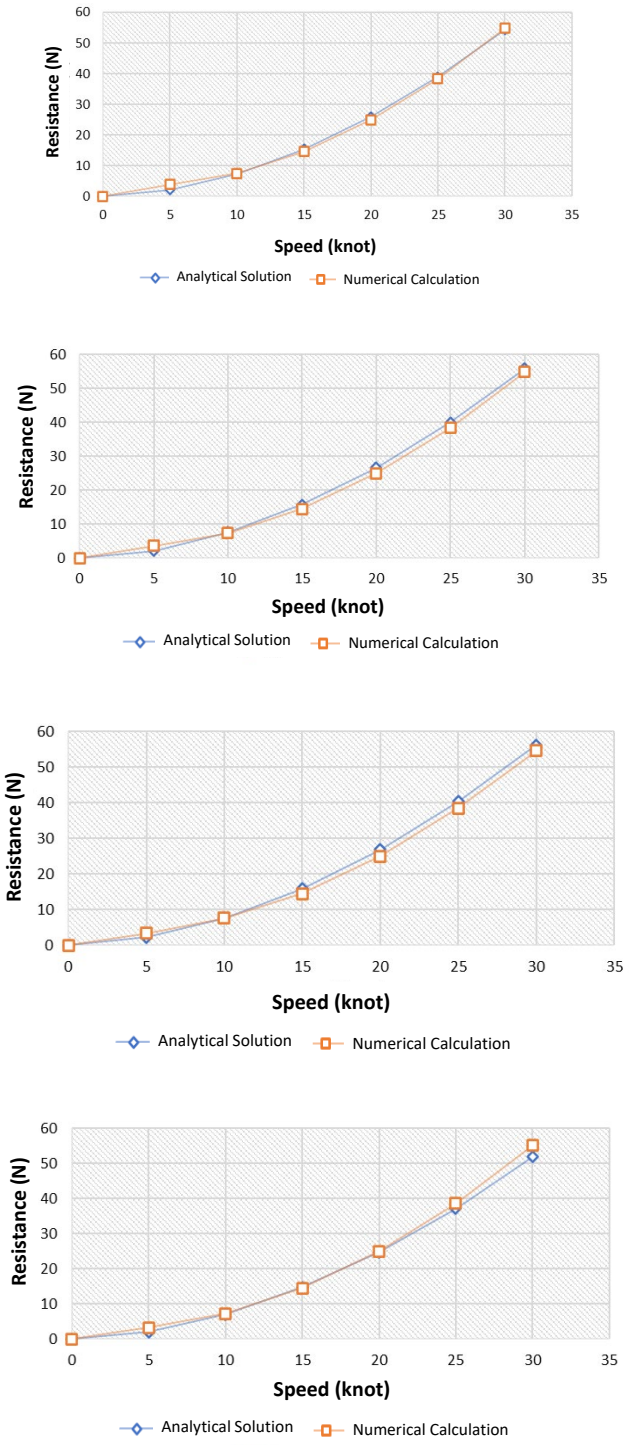

Fig. 6. Correlation speed with resistance planing catamaran.

Based on the data in Fig. 6(a), we found the highest resistance value at 30 knots speed of 53.26 N; in Fig. 6(b), the highest resistance is 54.31 N; in Fig. 6(c), the highest resistance is 55.82 N; in Fig. 6(d), the highest resistance is 56.17 N; and in Fig. 6(e), the highest resistance is 51.78 N. It can be stated that the most significant error at speeds of 5 knots was above 35%-50%.

4.2. Contours of the wave pattern

The configuration of the deadrise angle resulted in a change in the value of the resistance hull of the ship. The configuration of the deadrise angle also affected the wave pattern through the hull. As shown in Table 7, when the value of the Froude number was low, there were waves along the body of the ship. When the ship had a large deadrise angle, the waves that occurred around the ship were smoother.

However, when the Froude number of the ship entered the planing phase with a value of one, the change in the wave flow was not significant. In the catamaran, there were no significant changes that occurred in the wave pattern with the configuration of the deadrise angle (Table 8) when the Froude number was small or when the ship entered the planing phase. When the ship entered the planing phase, the waves that occurred around the ship looked smoother.

Table 7. Wave pattern of the designed monohull.
The wave pattern data is presented in Appendix A.

Deadrise Angle (°)	Froude Number	
	0.3	1
10	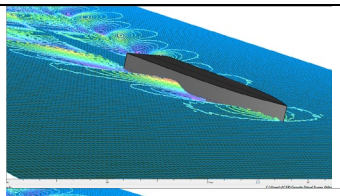	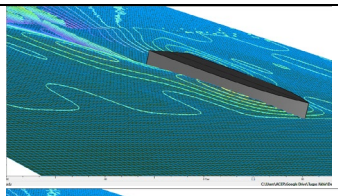
15	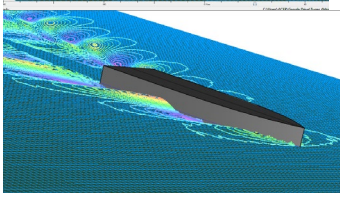	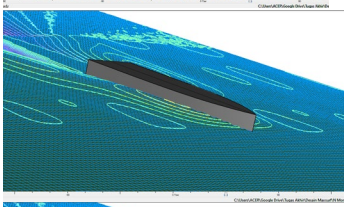
20	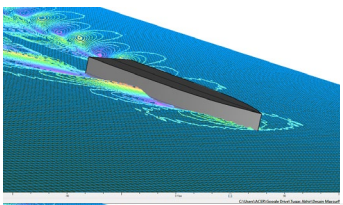	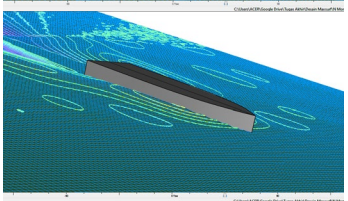
25	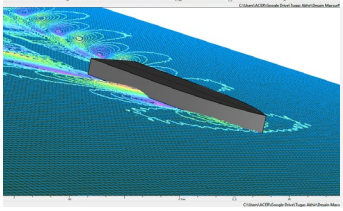	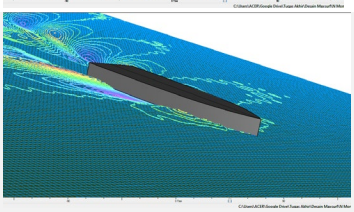

30	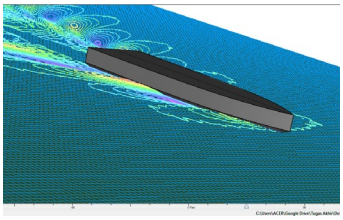	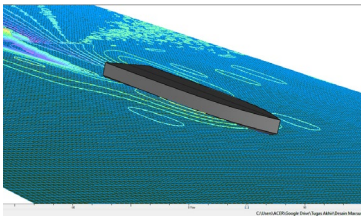

Table 8. Wave pattern of the designed catamaran. The wave pattern data is presented in Appendix B.

	Froude Number	
Deadrise Angle (°)	**0.3**	**1**
10	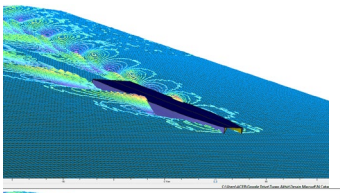	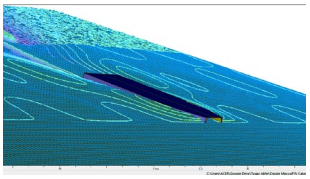
15	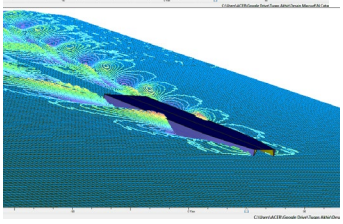	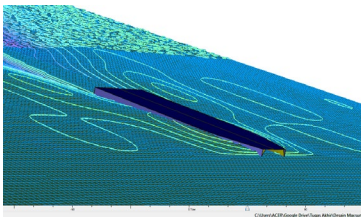
20	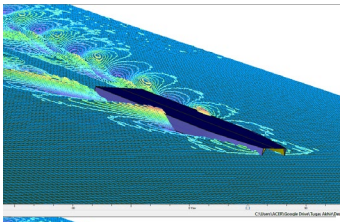	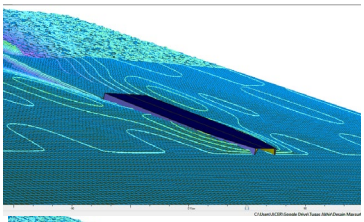
25	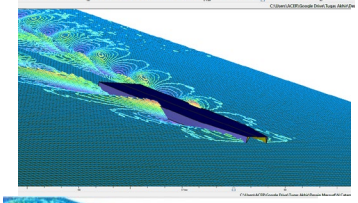	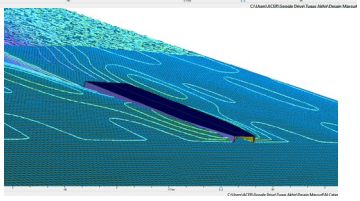
	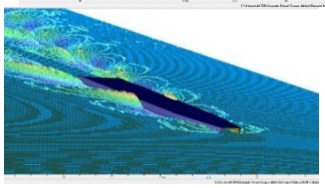	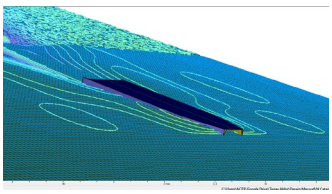

Theoretically, at a Froude number above 0.9, there was interference that minimized the wavelength so that the effect of the generated wavelength was less significant. The illustration regarding the wave and Froude number presented in Fig. 7 is referenced from the United States Naval Academy (USNA) [22]. Within distances of a few hull lengths, waves from all points on the hull surface will, in theory, contribute to the wave system. Some of the points are, however, more important than others, since the disturbance is larger. For a sailing yacht, the high pressure regions at the bow and stern are dominant, and it is usually assumed that only two wave systems exist (see the illustration in Fig 8).

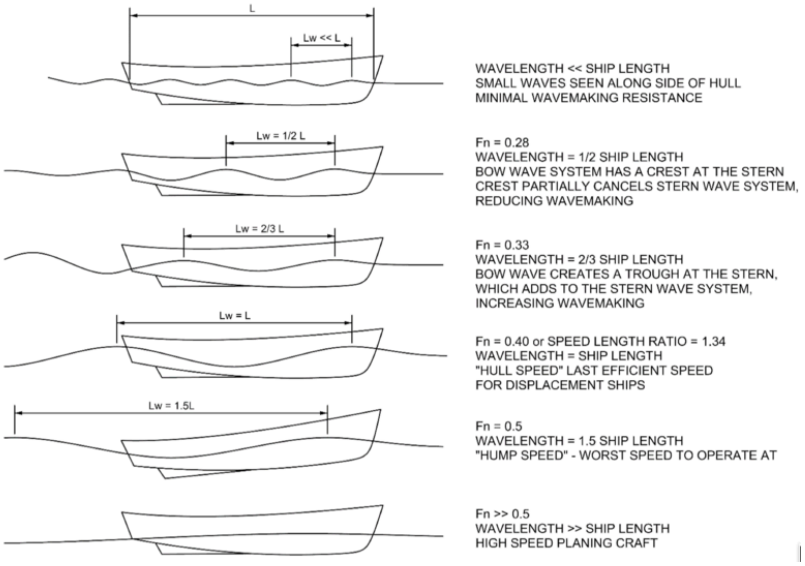

Fig. 7. Relation of the wavelength and Froude number in the theory of ship design.

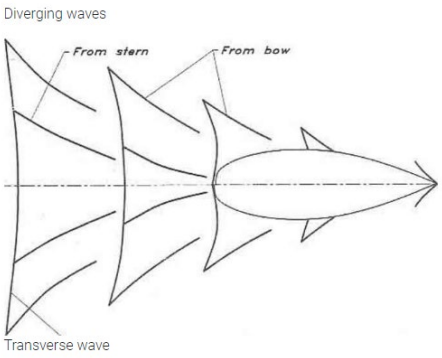

Fig. 8. Simplification of local bow and stern wave systems.

The speed dependence of the waves gives rise to an important phenomenon: interference. An illustration of this is given in Fig 9. If the wave crests from the bow system coincide with those from the stern, large waves will be created. On the other hand, if the bow wave crests coincide with troughs in the stern waves, the result is an attenuated wave. The first case is illustrated in (a) and (c), where the wavelengths are half and equal to the waterline length, respectively. In (b), the

wavelength of *Lwl* is 2A, and the waves are attenuated. In Fig. 9(d), the wavelength is larger than the *Lwl*.

The second wave crest then occurred aft of the stern, which, when the speed increased, moved into a trough, giving the hull a large trim angle. In each of the cases (a)-(d), a Froude number (*Fn*) exists (as discussed by Olivieri et al. in [34]) that determines how many waves there are along the hull. For instance, at *Fn* = 0.40, there was one wave; at 0.2, there were two; etc. The properties of the wave resistance curve were highly dependent on the Froude number. This study may be extended to a future work considering certain pioneering research [35-42] to investigate the effect of the wave resistance against *Fn* in developing the proposed hull models. Also, consideration to propulsion geometry (which is similar to turbine system [43-46]) is recommended to be studied as companion analysis in this subject. Several scholars in [47-49] have presented reference for this idea.

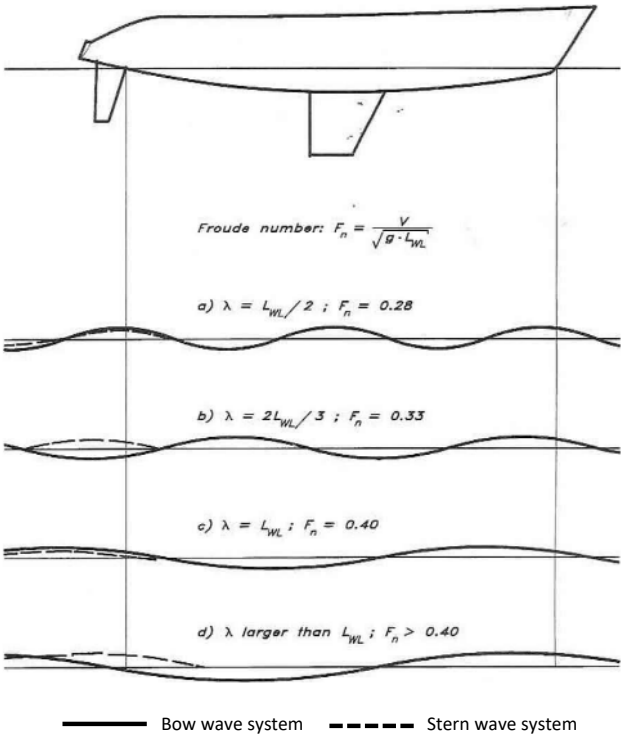

Fig. 9. Interference phenomenon on the wavelength.

5. Conclusions

This research was performed to investigate the effect on changes in the configuration of the deadrise angle on planing monohull and planing catamarans. The results of this study found an impact on the hull resistance and wave patterns with the conclusions below:

- The numerical results of the resistance characteristic were successfully validated using analytical solutions by deploying Savitsky's mathematical model. Similarity was confirmed to a satisfactory level for all proposed geometries and applied velocities.

- In monohull planing, we found that the hull resistance decreased by 16.87% at a 30° deadrise angle compared to the most significant resistance at any other deadrise angle.
- In catamaran planing, we found that the hull resistance decreased by 7.8% at a 30° deadrise angle compared to the most significant resistance at any other deadrise angle.
- This work will potentially be followed-up by future research considering larger deadrise angles to obtain the turning point of the angle with an effect on the resistance.
- The greatest error occurred at low speeds according to the Savitsky method used for high-speed vessels with a minimum Froude number of $F_n = 1$ and can be said to be high-density if $F_n > 1.2$.
- The total resistance obtained by monohull was smaller than the planing catamaran at 5.56 N (highest value among all results); one of the factors was the higher wetted surface compared to the catamaran planing.
- Changes in the angle of the deadrise angle affected the wave pattern around the monohull ship at a Froude number of 0.3; however, there was no significant effect on the catamaran.

Nomenclatures

B	Breadht, m
C_B	Block coefficient
C_F	Frictional resistance coefficient
C_M	Midship coefficient
C_P	Prismatic coefficient
Fr	Froude Number
g	Acceleration due gravity, m/s^2
L_{OA}	Length of ship overall, m
L_{WL}	Length on waterline, m
Re	Reynold number
R_F	Frictional resistance, N
R_T	Total resistance, N
R_V	Viscous resistance, N
R_W	Wave resistance, N
S	Surface wetted area, m^2
T	Draught, m
V	Speed, m/s
$(1+k)$	Form-factor, monohull
$(1+\beta k)$	Form-factor, catamaran
β	Deadrise angle, deg.
λ	Leeway angle, deg.
υ	Kinematic viscosity, m^2/s
ρ	Density of water, kg/m^3
τ	Trim angle, deg.
∇	Ship displacement volume, m^3
Δ	Ship displacement mass, tonnes

Acknowledgments

This work was supported by the RKAT PTNBH Universitas Sebelas Maret, Surakarta under Scheme of "Penelitian Unggulan UNS" (PU-UNS) - Year 2021, with

Grant/Contract No. 260/UN27.22/HK.07.00/2021. The support is gratefully acknowledged by the authors.

References

1. Nurkholis; Nuryadin, D.; Syaifudin, N.; Handika, R.; Setyobudi, R.H.; and Udjianto, D.W. (2016). The economic of marine sector in Indonesia. *Aquatic Procedia*, 7, 181-186.
2. Nuraini; Wahyuni, S.; Windiarto, T.; Oktavia, E.; and Karyono, Y. (2015). *Indonesian Population Profile 2015 SUPAS Results*. Central Bureau of Statistics-catalogue 2101033. Jakarta: Central Bureau of Statistics (in Indonesian).
3. Bappenas. (2019) *Technocratic Design of the 2020-2024 National Mid-Term Development Plan*. Jakarta: Ministry of PPN-Bappenas (in Indonesian).
4. Rustam, I. (2017). Kebijakan keamanan maritim di perbatasan Indonesia: Kasus kejahatan di Laut Sulawesi - Laut Sulu. *Jurnal Penelitian Politik*, 14(2), 165-181 (in Indonesian).
5. ICC - IMB (2019). *Piracy and Armed Robbery against Ships*. London: ICC International Maritime Bureau.
6. Doctors, L.J.; Day, A.H.; Clelland, D.; and Beveridge, P. (2010). Wave generation of a compartmented surface-effect ship. *Journal of Marine Science and Technology*, 15(4), 345-358.
7. Zhou, Z. (2003). *Theory and Analysis of Planing Catamarans in Calm and Rough Water*. Louisiana: University of New Orleans.
8. Lajeunesse, A. (2021). Canada's Arctic Offshore and Patrol Ships (AOPS): Their history and purpose. *Marine Policy*, 124, 104323.
9. Kim, D.J.; Kim, S.Y.; You, Y.J.; Rhee, K.P.; Kim, S.H.; and Kim, Y.G. (2013). Design of high-speed planing hulls for the improvement of resistance and seakeeping performance. *International Journal of Naval Architecture and Ocean Engineering*, 5(1), 161-177.
10. Liu, S.; and Papanikolaou, A. (2020). Regression analysis of experimental data for added resistance in waves of arbitrary heading and development of a semi-empirical formula. *Ocean Engineering,* 206, 107357.
11. Kim, G.H.; and Park, S. (2017). Development of a numerical simulation tool for efficient and robust prediction of ship resistance. *International Journal of Naval Architecture and Ocean Engineering*, 9(5), 537-551.
12. Wang, S.; Ji, B.; Zhao, J.; Liu, W.; and Xu, T. (2018). Predicting ship fuel consumption based on LASSO regression. *Transportation Research Part D: Transport and Environment*, 65, 817-824.
13. Farag, Y.B.A.; and Ölçer, A.I. (2020). The development of a ship performance model in varying operating conditions based on ANN and regression techniques. *Ocean Engineering.,* 198, 106972
14. Holt, P.; and Nielsen, U.D. (2021). Preliminary assessment of increased main engine load as a consequence of added wave resistance in the light of minimum propulsion power. *Applied Ocean Research*, 108, 102543.
15. Yan, L.; Jingyi, H.; and Kai, L. (2018). Hull form design optimization of twin-skeg fishing vessel for minimum resistance based on surrogate model. *Advances in Engineering Software*, 123, 38-50.

16. Khazaee, R.; Rahmansetayesh, M. A.; and Hajizadeh, S. (2019). Hydrodynamic evaluation of a planing hull in calm water using RANS and Savitsky's method. *Ocean Engineering*, 187, 106221.
17. Julianto, R.I.; Prabowo, A.R.; Putranto, T.; Adiputra, R.; and Muhayat, N. (2021). Investigation of hull design to quantify resistance criteria using Holtrop's regression-based method and Savitsky's mathematical model: A study case of fishing vessel. *Journal of Engineering Science and Technology*, 16(2), 1426-1443.
18. Elkafas, A.G.; Elgohary, M. M.; and Zeid, A. E. (2019). Numerical study on the hydrodynamic drag force of a container ship model. *Alexandria Engineering Journal*, 58(3), 849-859.
19. Doustdar, M. M.; and Kazemi, H. (2019). Effects of fixed and dynamic mesh methods on simulation of stepped planing craft. *Journal of Ocean Engineering and Science*, 4(1), 33-48.
20. Sun, H.; and Faltinsen, O. M. (2010). Numerical study of planing vessels in waves. *Journal of Hydrodynamics, Ser. B*, 22(5)Supplement 1, 468-475.
21. Molland, A.F.; Turnock, S.R.; and Hudson, D.A. (2017). *Ship Resistance, and Propulsion*. Cambridge: Cambridge University Press.
22. USNA. (2002). *Resistance and Powering of Ships*. Maryland: United States of Naval Academy.
23. Kristensen, H.O.; and Lützen, M. (2013). *Prediction of Resistance and Propulsion Power of Ships*. Project no. 2010-56, Work Package 2, Report no. 04, May 2013. Denmark: Technical University of Denmark-University of Southern Denmark.
24. Zeng, Q.; Hekkenberg, R.; Thill, C. (2019). On the viscous resistance of ships sailing in shallow water. *Ocean Engineering*, 190, 106434.
25. Schachter, R.D.; Ribeiro, H.J. C.; and Da Conceição, C.A.L. (2016). Dynamic equilibrium evaluation for planing hulls with arbitrary geometry and variable deadrise angles - The Virtual Prismatic Hulls Method. *Ocean Engineering*, 115, 67-92.
26. Kukner, A.; and Yasa, A.M. (2011). High speed planning hulls resistance prediction methods and comparasion. *Proceedings of the First International Symposium on Naval Architecturer and Maritime (INT-NAM)*. Istanbul, Turkey, 201-208.
27. Rehm, B.; Schubert, J.; Haghshenas, A.; Hughes, J.; and Paknejad, A.S. (2009). M*anaged Pressure Drilling*. Texas: Gulf Publishing Company.
28. Vitello, L.; Miranda, S.; Balsamo, F.; Bove, A.; and Caldarella, S. (2012). Stepped hulls: Model experimental tests and sea trial data. *Proceedings of the Seventeenth International Conference on Ships and Shipping Research (NAV)*, Naples, Italy.
29. Savitsky, D. (1964). Hydrodynamic design of planing hulls. *Marine Technology*, 1(1), 71-95.
30. Bentley. (2013). *Maxsurf Resistance*. Pennsylvania: Bentley Systems, Inc.
31. Park, C.H.; Park, H.S.; Jang, H.Y.; and Im, N. (2014). A comparison study on the deck house shape of high speed planing crafts for air resistance reduction. *International Journal of Naval Architecture and Ocean Engineering*, 6(4), 867-875.

32. Yousefi, R.; Shafaghat, R.; and Shakeri, M. (2014). High-speed planing hull drag reduction using tunnels. *Ocean Engineering*, 84, 54-60.
33. Liu C.Y.; and Wang, C. T. (1979). Interference effect of catamaran planing hulls. *International Journal of Hydronautics*, 13, 31-32.
34. Olivieri, A.; Pistani, F.; Wilson, R.; Benedetti, L.; Gala, F.L.; Campana, E.F.; and Stern, F. (2004). *Froude Number and Scale Effects and Froude Number 0.35 Wave Elevations and Mean-Velocity Measurements for Bow and Shoulder Wave Breaking of Surface Combatant DTMB 5415.* Iowa: University of Iowa.
35. Wang, Z.; and Lu, X.P. (2011). Numerical simulation of wave resistance of trimarans by nonlinear wave making theory with sinking and trim being taken into account. *Journal of Hydrodynamics, Ser. B*, 23(2), 224-233.
36. Baree, M.S.; Afroz, L.; and Sakib, S. (2017). An experiment with a ship model for prediction of added resistance in waves. *Procedia Engineering*, 194, 90-95.
37. Julianto, R.I.; Muttaqie, T.; Adiputra, R.; Hadi, S.; Hidajat, R.L.L.G.; Prabowo, A.R. (2020). Hydrodynamic and structural investigations of catamaran design. *Procedia Structural Integrity*, 27, 93-100.
38. Abbasnia, A.; and Soares, C.G. (2019). Fully nonlinear and linear ship waves modelling using the potential numerical towing tank and NURBS. *Engineering Analysis with Boundary Elements*, 103, 137-144.
39. Huang, L.; Tuhkuri, J.; Igrec, B.; Li, M.; Stagonas, D.; Toffoli, A.; Cardiff, P.; Thomas, G. (2020). Ship resistance when operating in floating ice floes: A combined CFD&DEM approach. *Marine Structures*, 74, 102817.
40. Terziev, M.; Tezdogan, T.; and Incecik, A. (2019). A geosim analysis of ship resistance decomposition and scale effects with the aid of CFD. *Applied Ocean Research*, 92, 101930.
41. Luo, S.; Ma, N.; and Yoshiaki, H. (2016). Evaluation of resistance increase and speed loss of a ship in wind and waves. *Journal of Ocean Engineering and Science*, 1(3), 212-218.
42. Bahatmaka, A.; Kim, D.J.; Prabowo, A.R.; and Zaw, M.T. (2018). Investigation on the performance of the traditional Indonesian fishing vessel. *MATEC Web of Conferences*, 159, 02056.
43. Prabowoputra, D.M.; Hadi, S.; Sohn, J.M.; and Prabowo, A.R. (2020). The effect of multi-stage modification on the performance of Savonius water turbines under the horizontal axis condition. *Open Engineering,* 10(1), 793-803.
44. Prabowoputra, D.M.; Prabowo, A.R.; Hadi, S.; and Sohn, J.M. (2021). Assessment of turbine stages and blade numbers on modified 3D Savonius hydrokinetic turbine performance using CFD analysis. *Multidiscipline Modeling in Materials and Structures,* 17(1), 253-272.
45. Prabowo, A.R.; and Prabowoputra, D.M. (2020). Investigation on Savonius turbine technology as harvesting instrument of non-fossil energy: Technical development and potential implementation. *Theoretical and Applied Mechanics Letters,* 10(4), 262-269.
46. Prabowoputra, D.M.; Hadi, S.; Prabowo, A.R.; and Sohn, J.M. (2020). Performance investigation of the savonius horizontal water turbine accounting for stage rotor design. *International Journal of Mechanical Engineering and Robotics Research*, 9(2), 184-189.

47. Yusvika, M.; Prabowo, A.R.; Baek, S.J.; and Tjahjana, D.D.D.P. (2020). Achievements in observation and prediction of cavitation: Effect and damage on the ship propellers. *Procedia Structural Integrity*, 27, 109-116.
48. Yusvika, M.; Prabowo, A.R.; Tjahjana, D.D.D.P.; and Sohn, J.M. (2020). Cavitation prediction of ship propeller based on temperature and fluid properties of waters. *Journal of Marine Science and Engineering,* 8 (6), 465.
49. Bahatmaka, A.; Kim, D.J.; Chrismianto, D.; Setiawan, J.D.; and Prabowo, A.R. (2017). Numerical investigation on the performance of ducted propeller. *MATEC Web of Conferences*, 138, 07002.

Appendix A

Wave Pattern of the Monohull Designs based on Resistance Analysis

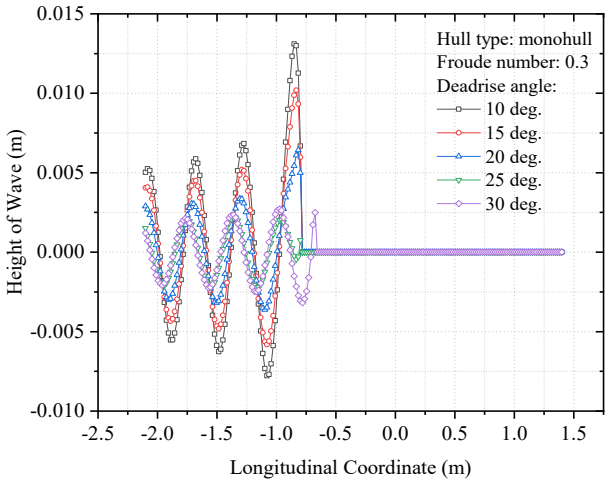

Fig. A-1. Generated wave pattern of the proposed monohull with *Fn* = 0.3.

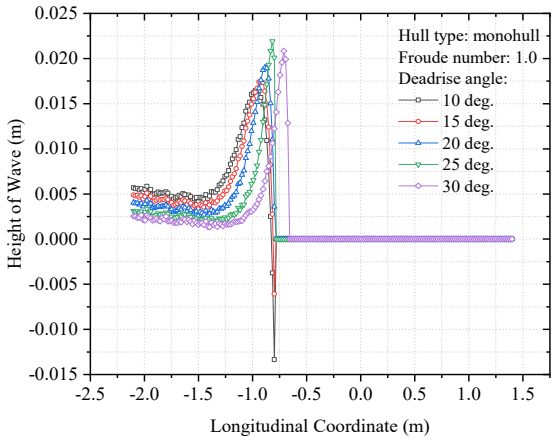

Fig. A-2. Generated wave pattern of the proposed monohull with *Fn* = 1.

Appendix B

Wave Pattern of the Monohull Designs based on Resistance Analysis

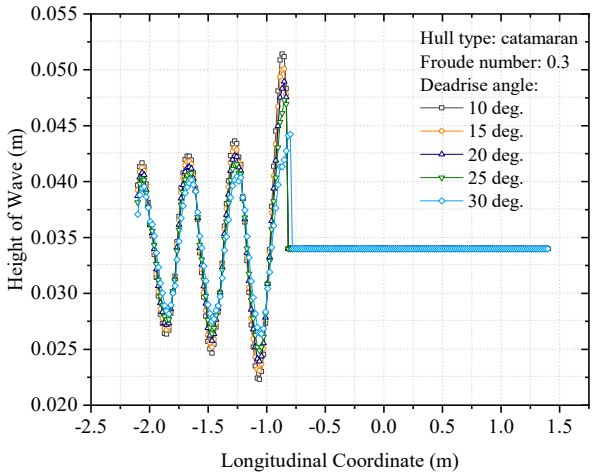

Fig. B-1. Generated wave pattern of the proposed catamaran with *Fn* = 0.3.

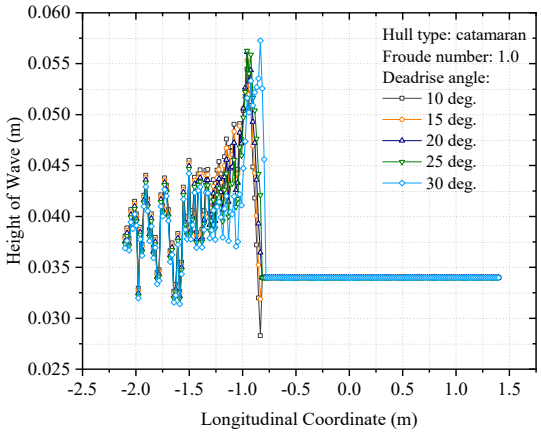

Fig. B-2. Generated wave pattern of the proposed catamaran with *Fn* = 1.